ECS Transactions, 68 (1) 2285-2293 (2015)
10.1149/06801.2285ecst ©The Electrochemical Society

Investigation of 2R-cell Degradation Under Thermal Cycling and RedOx Cycling Conditions by Electrochemical Impedance Spectroscopy

S. Diethelm, V. Singh, J. Van herle

FuelMAT Group, Institute of Mechanical Engineering (IGM), Faculty of Engineering (STI), École Polytechnique Fédérale de Lausanne (EPFL) 1015 Lausanne, Switzerland

A 2R-cell with a 10 cm^2 active area LSCF cathode on a CGO buffer layer was tested at 780°C under thermal and RedOx cycling conditions; 20 thermal cycles were performed between 780°C and 100°C, using 200°C/h heating ramps and natural cooling, followed by 20 RedOx cycles, during which air was fed to the anode for 1 hour at 780°C, causing the cell potential to drop to zero. V-i polarisation curves and electrochemical impedance spectroscopy (EIS) measurements were performed before and after each consecutive cycle in order to monitor the performance losses. The OCV remained stable during the whole test whereas the area specific resistance (ASR) measured at 0.5 A/cm^2 increased by +1.3 $m\Omega cm^2$ per thermal cycle and by +1.8 $m\Omega cm^2$ per RedOx cycle. The cell was examined after the test by scanning electron microscopy (SEM).

Introduction

The prevalent anode supported thin electrolyte solid oxide fuel cells (ASC) used today are highly susceptible to failure under RedOx conditions. The expansion caused during the oxidation of Ni to NiO can destroy the support, leading to irreversible cell damage. Many solutions have been investigated to solve this problem. Amongst the material related solutions, one can mention the modification of the cell microstructure (particle size distribution, controlled porosity, lowering of Ni-content, etc.), the development of alternative anode materials (Ni alloying, full ceramic anodes, etc.) and slowing of the Ni reoxidation kinetics (1). To counter this problem, Fiaxell SOFC Technologies (Switzerland) has engineered the microstructure of their cells to confer added RedOx stability to their anode supported cell (2R-cell™) (2).

In this study a 2R commercial cell was investigated against thermal and RedOx cycling. Electrochemical impedance spectroscopy (EIS) was used to identify the changes occurring during the cycling of the cell and the underlying mechanisms.

Experimental

The cell used in this study is a RedOx-stable 2R anode supported cell from Fiaxell (∅60mm, 10 cm^2 active area) with a 20CGO barrier layer and a LSCF ($La_{0.6}Sr_{0.4}Co_{0.2}Fe_{0.8}O_{3-\delta}$) cathode. The anode support was sintered at 1380°C for 6 hours. The ceria barrier layer was sintered 3 hours at 1200°C with 2% CoO as a sintering aid. The cathode is composed of two layers of LSCF sintered 2 hours at 1000°C. The cell was

tested in a metallic set-up with open flanges, which is schematically depicted in Figure 1. A gold mesh was used as the current collection on the cathode side, and Ni-foam on the anode side, with gold wires for current leads and voltage probes. A K-type thermocouple was positioned next to the cathode. The cell and current collectors were compressed together between spring-loaded flanges using alumina felt insulating layers. The assembly was placed in the middle of a furnace (Rohde). The gas supply was controlled by MFCs (Red-y, Voegtlin).

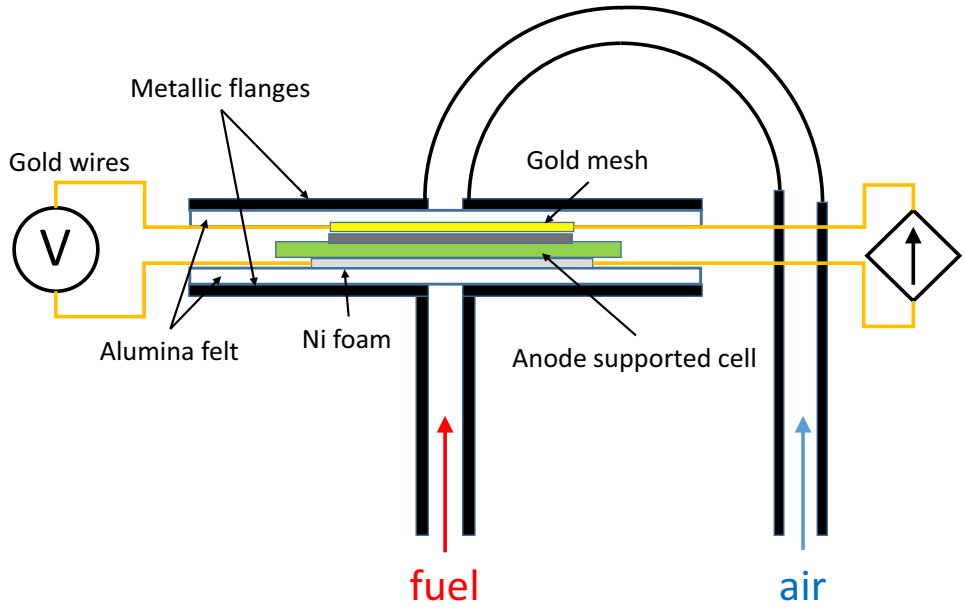

Figure 1. Schematic representation of the cell assembly in the open-flange set-up.

Prior to testing, the cell was reduced at 800°C. The cell was therefore heated in air up to 800°C. The anode compartment was then purged with Ar, then fed with 20%H_2 in Ar, before switching to 100%H_2. 500Nml/min air was fed to the cathode and 180Nml/min dry hydrogen to the anode. After a stabilization period of ~70h, thermal cycles were performed during 700h. Therefore, the fuel was changed to 1/3H_2 with 2/3Ar keeping the same total flow and the furnace was stopped for 10 hours during which the cell temperature dropped down to 100°C. The cell was then reheated using a 200°C/h heating ramp back to 780°C. The fuel composition was changed back to 100% H_2 and the cell characterised by DC-polarization curve (V-i) and EIS. This cycle was repeated 20 times. After that, RedOx-cycles were performed; after EC characterisation (V-i, EIS), the cell was set at OCV, the anode compartment was first purged with Ar and then fed with air for one hour during which the cell voltage dropped below 20mV. The cell was then reduced again and characterized. Between each RedOx cycles, the cell was polarized at 0.5A/cm^2 for ~24h.

All electrochemical measurements were performed with a IM6 workstation coupled with a power potentiostat PP240 from Zahner Elektrik. EIS measurements were performed in the 50k-50mHz frequency range, with a 10mA/cm^2 perturbation amplitude at 0.5A/cm^2 current bias. All EIS measurements were smoothed using Thales software (Zahner) and the high frequency parasitic inductance was corrected using the procedure described by B. Liu *et al.* (3) in order to get an improved estimate of the ohmic resistance.

Results and Discussion

Thermal Cycling

Figure 2 shows the evolution of the cell area specific resistance (ASR) after 20 consecutive thermal cycles. The ASR was calculated from the V-i curves taking the slope around 0.5±0.05 A/cm^2. A monotonous increase of the ASR of 1.3 mΩcm^2 per cycle is observed. Figure 2 also shows the total cell resistance (Rt) calculated from the EIS measurements performed after each thermal cycle at 0.5A/cm^2 bias. The agreement between both measurements is good as expected. Distinguishing between the serial (Rs) and the polarisation (Rp) resistance, one obtains respectively an increase of 0.8 and 0.6 mΩcm^2 per cycle. Thereby the degradation is mainly ohmic, which relates to the changes in conductivity of the cell layers or the contacts between them.

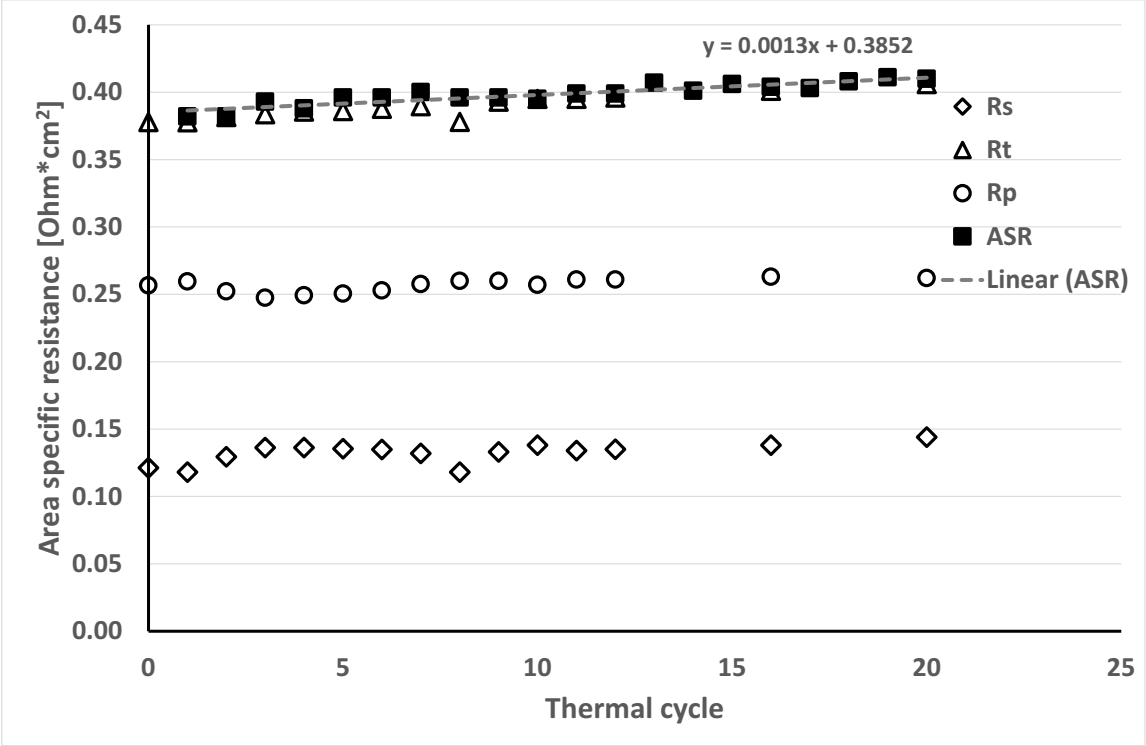

Figure 2. Evolution after consecutive thermal cycles of the cell ASR measured from the slope of the V-i curves around 0.5A/cm^2. The total cell resistance (Rt), the serial (Rs) and the polarization (Rp) resistances are obtained from the EIS measurement at 0.5A/cm^2 bias.

More information about the increase of the polarisation resistance upon thermal cycling can be obtained by looking at the frequency dispersion of the imaginary part of the cell impedance. Figure 3 shows the imaginary part of EIS data plotted in a Bode-plot vs. the frequency, measured after consecutive thermal cycles. It can be observed that the impedance increase with thermal cycling affects principally the low frequency region of the spectra (peak around 3Hz), whereas in the high frequency region (>30Hz), the impedance diminishes, corresponding to an improvement of the performance upon cycling.

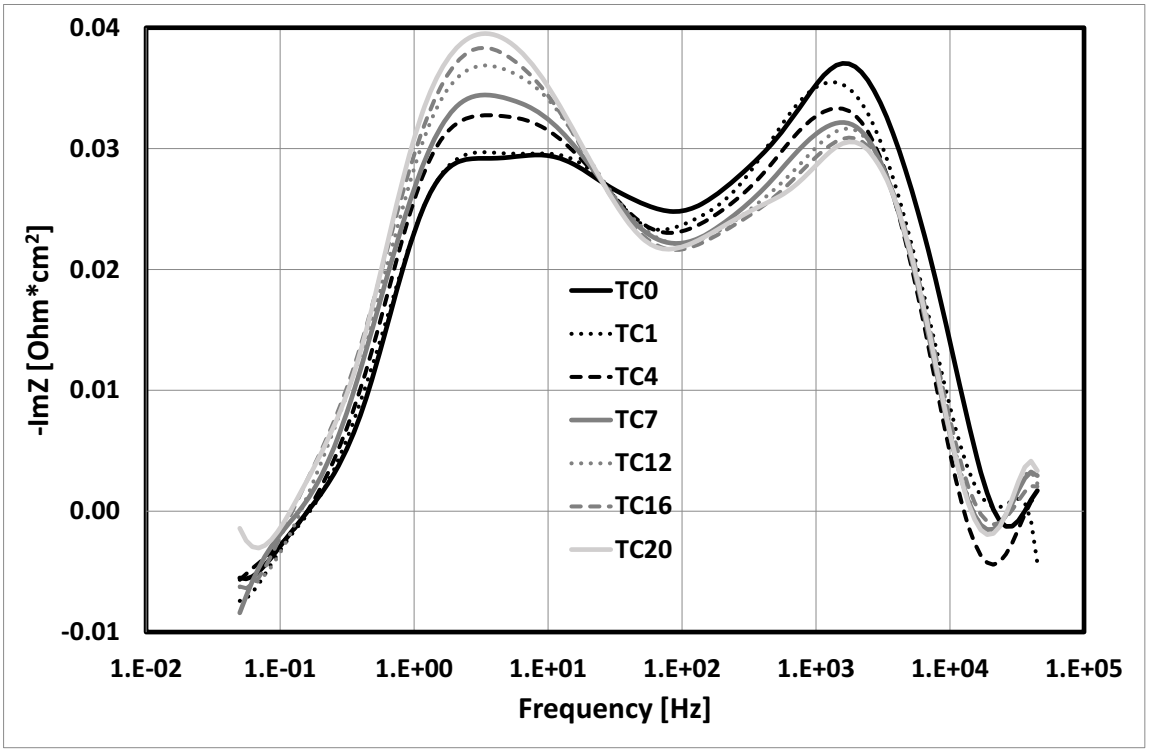

Figure 3. Bode plot of the imaginary part of the cell impedance measured after consecutive thermal cycles.

The picture can be further refined by subtracting the initial performance of the cell prior to thermal cycling. This is shown in Figure 4. The values that appear as positive correspond to a degradation compared to the initial performance of the cell, whereas those that are negative correspond to an improvement. The features already mentioned regarding Figure 3 appear clearly in Figure 4: at low frequencies, two peaks can be identified at respectively 0.5Hz and 3Hz. Both gradually increase, meaning that they correspond to processes becoming more and more limiting upon thermal cycling and thereby contribute to the overall increase of the polarization resistance. Processes occurring at such low frequencies are usually attributed to gas conversion or gas transport limitations (4,5). Sensitivity tests were performed on the same cell by varying the H_2 concentration on the anode side and the oxygen concentration on the cathode side. The 3Hz process seems to be more consistent with gas transport in the anode whereas the 0.5Hz peak could be attributed to both sides. Nevertheless, this means that the degradation related to the increase of the polarisation resistance could stem from changes in the porosity of the electrodes (grain coarsening, densification…).

Now considering the high frequency part of the spectrum, three peaks at respectively 60Hz, 1kHz and 10kHz can be identified in Figure 4, all of them negative, i.e. corresponding to an improvement compared to the initial performance of the cell. The peak around 1kHz showed strong dependence upon current and varied with fuel composition. It is therefore meaningful to attribute it to the anodic charge transfer (4,5). For the interpretation of the two other peaks, more experiments and analyses are necessary.

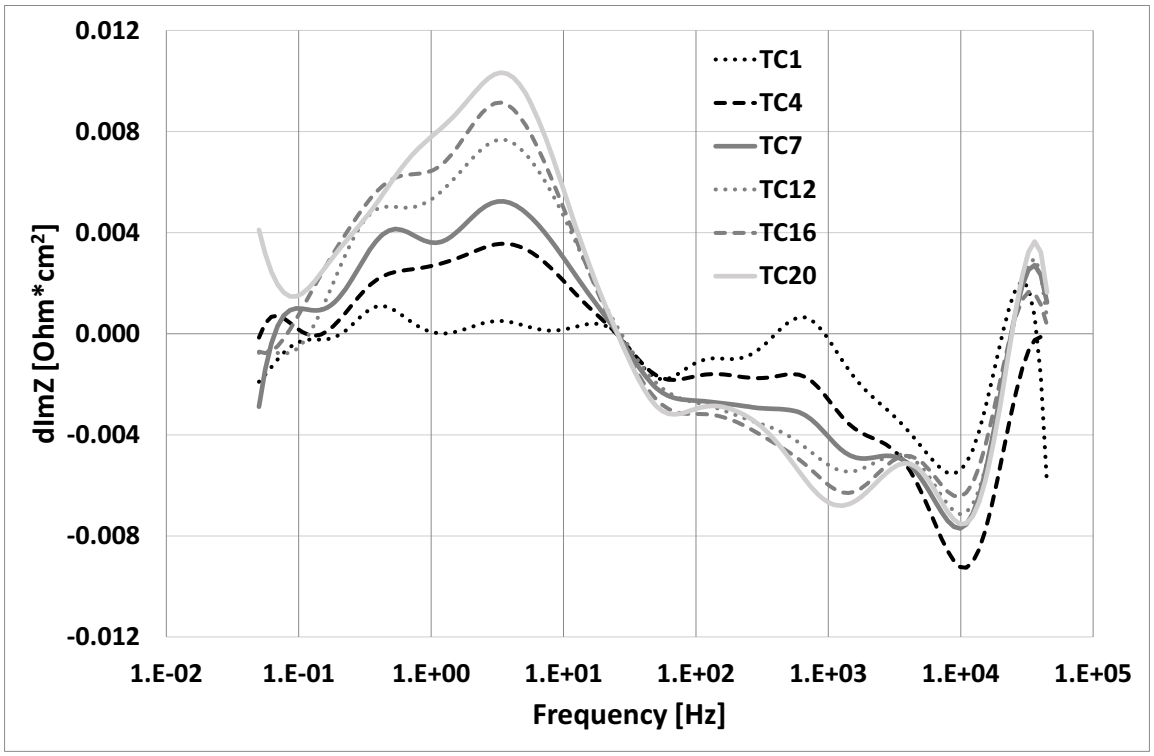

Figure 4. Bode plot of the difference between the imaginary part of the cell impedance after consecutive thermal cycles and the cell impedance prior to thermal cycling (-ImZ(TCNr)+ImZ(TC0)).

RedOx-Cycling

Following the thermal cycling, 20 RedOx cycles were performed on the same cell. V-i characterisation was performed directly after the RedOx cycle (i) and after a stabilization period (f) of ~24h during which the cell was polarized at 0.5A/cm^2. The cell performances were systematically better just after the RedOx-cycle and then decayed rapidly to reach a new stable value. The ASRs calculated from the V-i curves after stabilization are given versus the number of RedOx-cycles in Figure 5. The degradation rate per RedOx cycle obtained from a linear regression is 1.8 mΩcm^2/cycle. Converted in terms of cell voltage, this degradation corresponds to 2.7 mV/cycle, leading to 6% overall degradation for 20 cycles. As for the thermal cycles, the total cell resistance (Rt) was also calculated from EIS measurements performed after stabilization at 0.5A/cm^2 current bias. The values of Rt are similar to the ASR values, although slightly lower. However, the corresponding degradation rate per RedOx cycle is much smaller, i.e. 0.8 mΩcm^2/cycle vs. 1.8 mΩcm^2/cycle. As previously, the serial (Rs) and polarisation (Rp) were distinguished and are also shown in the same figure. In this case, according to the EIS data, the main contribution to the cell degradation upon RedOx cycling comes from the polarisation losses, i.e. 0.7 mΩcm^2/cycle against only 0.1 mΩcm^2/cycle for the ohmic losses.

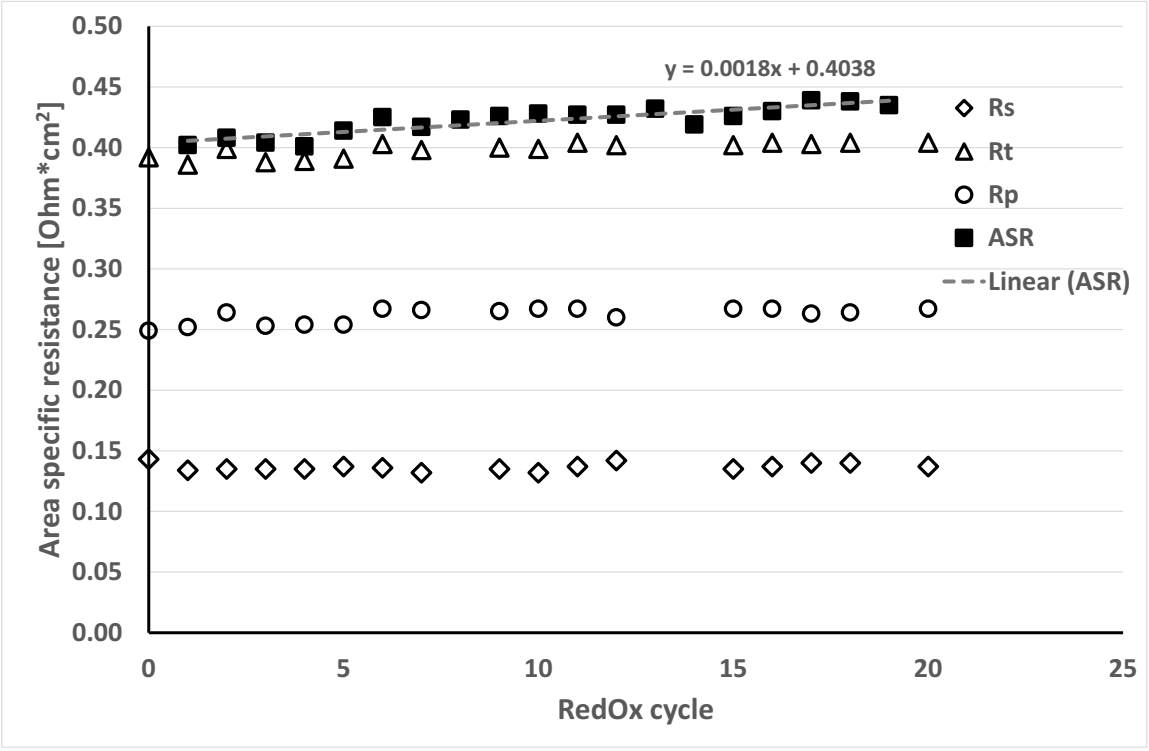

Figure 5. Evolution after consecutive RedOx cycles of the cell ASR measured from the slope of the V-i curves around 0.5A/cm^2. The total cell resistance (Rt), the serial (Rs) and the polarization (Rp) resistances are obtained from the EIS measurement at 0.5A/cm^2 bias.

Looking at the EIS data, especially at the Bode plot (Figure 6), one observes clearly the effect of the RedOx cycle: immediately after the cycle (i), the high frequency peak (~5kHz) is reduced, whereas the low frequency peak (~3Hz) increases. On the contrary, after the stabilization period (f), the high frequency peak increases again, whereas the low frequency peak decreases. This cyclic re-activation after the RedOx cycle and the gradual de-activation during stabilization occurs for each RedOx cycle, although the difference at high frequency between the final and the initial state tends to diminish upon RedOx cycling, whereas the difference at low frequency (1-3Hz) increases and shifts to higher frequencies. Both effects can relate to a modification of the anode functional layer (AFL): after the RedOx-cycle, the Ni grains are fragmented and redistributed, thereby improving the conductivity and increasing the triple phase boundary (TPB) but hindering the gas supply to the electrochemically active area. During the stabilization, Ni grain coarsening occurs, reducing the conductivity and activity of the AFL but at the same time increasing its porosity (6).

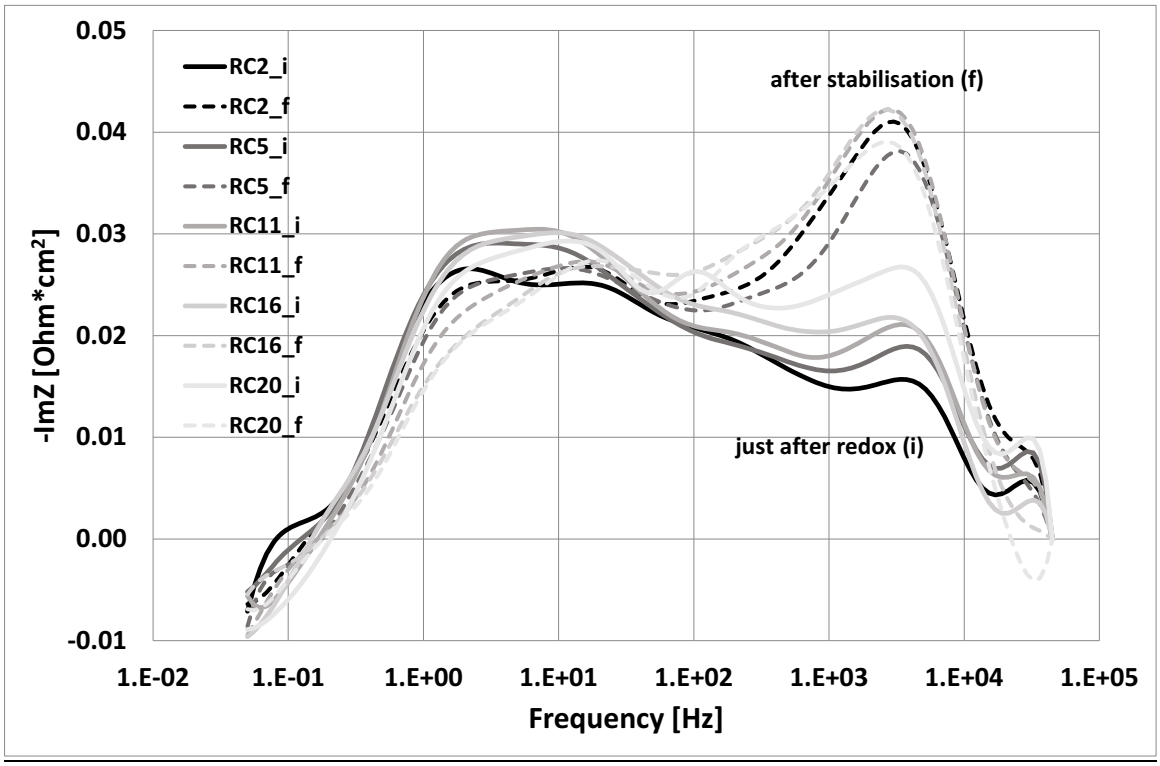

Figure 6. Bode plot of the imaginary part of the cell impedance measured after consecutive RedOx cycles. The (i) refers to the initial state just after the RedOx cycle, whereas the (f) refers to the final state after 24h stabilization.

Figure 7 shows the changes that occur in the polarization losses upon RedOx cycling. It compares in a Bode plot the difference between the performance of the cell prior to cycling and after stabilization (f) consecutive to RedOx cycles. As in Figure 4, there is a negative portion of the spectrum, corresponding to a gradual improvement, and a positive portion corresponding to degradation, but this time the trend is opposite. There is one main negative peak at 1Hz, corresponding to gas conversion and transport (4,5) that becomes more and more negative upon cycling, indicating that gas transport to the anode is improving. On the other hand, two positive peaks are visible around respectively 300Hz and 3kHz. As mentioned previously, both peaks showed sensitivity upon fuel composition and the higher frequency peak varied with current bias. The former is probably related to H_2 diffusion in the AFL whereas the latter is linked to the anodic charge transfer reaction. Both point towards changes in the AFL microstructure.

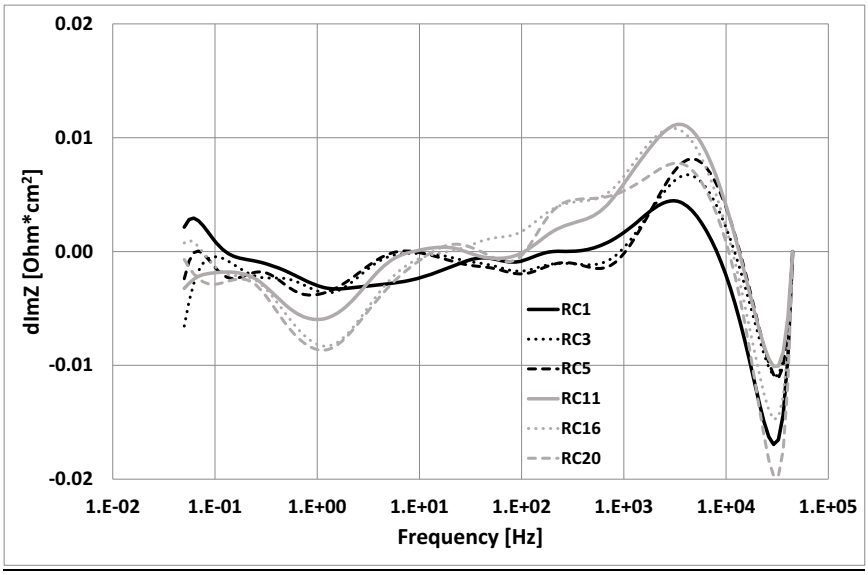

Figure 7. Bode plot of the difference between the imaginary part of the cell impedance after stabilization consecutive to RedOx cycles and the cell impedance prior to cycling (-ImZ(RCNr_f)+ImZ(RC0)).

Post-test SEM Examination

At the end of the test, the cell was re-oxidized and cooled down for post-test examination. The cell was broken and the cross-section was examined by scanning electron microscopy (SEM). No delamination was observed at the CGO/cathode interface nor the CGO/YSZ interface as seen in Figure 8. However, the anode functional layer that appears on the bottom of the micrograph presents a crumbled aspect, probably resulting from the repeated RedOx-cycles. This observation correlates well with the discussion of Figures 6 and 7.

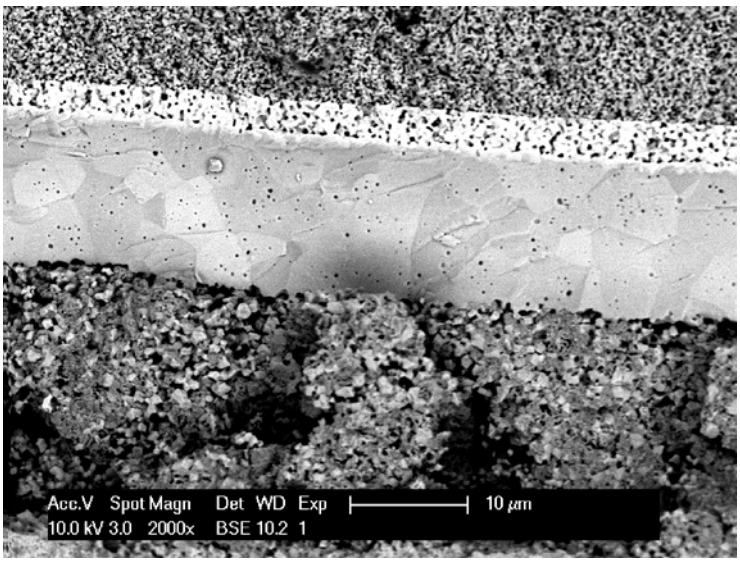

Figure 8. Back-scattered electron micrograph of the 2R cell cross section after the thermal and RedOx cycling tests (in oxidized state). From top to bottom, one distinguishes part of the cathode, the GDC layer, the YSZ electrolyte and the anode functional layer.

Conclusions

20 thermal cycles between 100 and 780°C were performed on a 2R-cell from Fiaxell with +1.3mΩcm^2/cycle ASR degradation. EIS measurements showed that the degradation was mainly due to an increase of the ohmic losses (0.8 mΩcm^2/cycle). Besides, the main contribution to the polarization resistance increase was related to gas transport limitation resulting from changes in the electrodes porosity (grain coarsening, densification).

20 RedOx cycles were also achieved with the same cell, showing only +1.8mΩcm^2/cycle of ASR degradation. A performance improvement was observed immediately after the RedOx cycle, attributed to Ni grains fragmentation and redistribution, thereby increasing the TPB. This was followed by a performance decrease during a stabilization period attributed to Ni grains recoarsening. Considering the performance after stabilization, the degradation upon RedOx cycling was mainly due to polarization losses, attributed to changes in the AFL microstructure. This degradation corresponds to an overall cell voltage degradation (at 0.5 A/cm^2) of 6% after 20 RedOx-cycles, i.e. only 0.3% per RedOx cycle.

Acknowledgments

This study was supported by the State Secretariat for education, Research and Innovation (SERI) through the EUROSTARS project E!7565 ROXSOLIDCELL.

References

1. A. Faes, RedOx stability of anode supported solid oxide fuel cells, PhD thesis, Ecole Polytechnique Fédérale de Lausanne, Thesis Nr 4893 (2011), pp. 2.53-86.
   A. Faes, A. Hessler-Wyser, A. Zryd, J. Van herle, *Membranes*, **2 (3),** 585-664 (2012**).**
2. Di Domenicantonio, Giulia; Briois, Pascal; Billard, Alain; *et al.*, *ECS Trans.*, **57 (1)**, 867 (2013).
3. B. Liu, H. Muroyama, T. Matsui, K. Tomida, T. Kabata, K. Eguchia, *J. Electrochem. Soc.*, **157 (12)**, B1858-B1864, (2010).
4. R. Barfod, M. Mogensen, T. Klemensoe, A. Hagen, Y-L. Liu, P. V. Hendriksen, *J. Electrochem. Soc.*, **154 (4)**, B371-B378, (2007).
5. A. Leonide, V. Sonn, A. Weber, E. Ivers-Tiffée, *J. Electrochem. Soc.*, **155 (1)**, B36-B41, (2008).
6. A. Faes, A. Hessler-Wyser, D. Presvytes, C. G. Vayenas, J. Van herle, *Fuel Cells*, **9 (6)** 841-851, (2009)